

Dynamic voltage restorer based on particle swarm optimization algorithm and adaptive neuro-fuzzy inference system

Saddam Subhi Salman, Abdulrahim Thiab Humod, Fadhil A. Hasan

Department of Electrical Engineering, University of Technology, Baghdad, Iraq

Article Info

Article history:

Received Apr 30, 2022

Revised Aug 8, 2022

Accepted Aug 31, 2022

Keywords:

ANFIS
Dynamic voltage restorer
Particle swarm optimization
Power quality
Voltage sag
Voltage swell

ABSTRACT

This article uses a dynamic voltage restorer to tackle a wide range of power quality issues, such as voltage drooping and swelling, spikes, distortions, and so on. The proportional controller, integrated controller (PI), and adaptive neuro-fuzzy inference system (ANFIS) are proposed dynamic voltage restorer (DVR) controllers. The control strategy's goal is to employ an injection transformer to mitigate for the needed voltage and keep the load voltage fixed. The settings of the PI controller are fine-tuned using two methods: trial and error and intelligent optimum. Particle swarm optimization (PSO) is now the most effective method. In terms of settling time, overshoot, undershoot, and disturbances around the final value, the PSO-tuned PI controller outperforms the trial-and-error PI controller. The ANFIS controller is used to regulate the DVR's responsiveness through the PI-PSO controller. The PI-PSO data is used as training data by the ANFIS controller. The results show that a DVR with an ANFIS controller outperforms a PI-PSO controller in terms of overshoot, undershoot spike voltage, steady state time, and settling time. In the case of a failure voltage, the DVR with an ANFIS controller has a 27% undershoot spike voltage while the PI-PSO controller has a 30% undershoot spike voltage.

This is an open access article under the [CC BY-SA](https://creativecommons.org/licenses/by-sa/4.0/) license.



Corresponding Author:

Saddam Subhi Salman
Department of Electrical Engineering, University of Technology
6001 Alsanana, Baghdad, Iraq
Email: eee.20.53@grad.uotechnology.edu.iq

1. INTRODUCTION

With the widespread usage of voltage-sensitive load devices in today's distribution networks, power quality issues such as transients, droops, and swelling are becoming increasingly dangerous. A dynamic voltage restorer (DVR) is a device that protects critical loads from various types of interruptions. Figure 1 depicts the fundamental notion of a DVR. The DVR should be able to discern voltage sag and manage the inverter to precisely and quickly restore the voltage [1]–[4]. A dynamic voltage restorer (DVR) is a strong power electronics controller with a quick reaction time that provides variable voltage regulation at the point of connection to the electrical distribution systems, resulting in improved power quality. The DVR has emerged as a viable technology for solving additional power quality issues such as flicker reduction, power factor correction, and harmonics management, in addition to voltage regulation improvement [5]–[8]. Voltage sag occurs when the voltage suddenly drops to 10–90% of the supplied voltage. The abrupt rise in load over that specific feeder is the source of this. In contrast, a voltage swelling is described as a sudden rise in voltage that exceeds 110% of the supply voltage. This is due to a rapid decrease in the load on that specific feeder. When there is a voltage rise or reduction, the voltage is corrected by inserting it in series with the supply from another feeder using a DVR [9]–[12]. Various techniques are available for mitigating the effect of voltage disruptions on critical loads. Using power electronic devices as compensators is the most efficient

and adaptable method. These compensators are known as bespoke power devices and comprise serial, parallel, and series-parallel compensators. Serial compensators, such as the static series compensator (SCC), dynamic voltage compensator (DVC), and DVR, are thought to be the most cost-effective methods for voltage compensation in distribution networks [13]–[16]. DVRs are series-connected devices that are used to address voltage-related power quality concerns such as voltage sag, swelling, and total harmonic distortion (THD) reduction. A DVR is a bespoke power device that injects or absorbs three-phase AC electricity in synchrony with the voltage of a distribution feeder [4], [17]. A DVR is a device that uses a boosting transformer to insert a dynamically regulated voltage in series with the bus voltage, as shown in Figure 1. Three single-phase boosting transformers are linked to a three-phase converter that includes an energy storage system and a control circuit. The magnitude of the three injection phase voltages is adjusted to avoid any negative effects on the load voltage caused by a bus failure. This implies that any voltage difference produced by transient disruptions in the AC feeder will be balanced by an equivalent voltage produced by the converter and supplied at the medium voltage level via the boosting transformer [18]–[20]. The DVR's topology was used as an active series filter to improve voltage stability, reduce harmonics, mitigate any reactive power deficit, and improve energy sustainability [21]. In this paper, a dynamic voltage restorer device is proposed to compensate for the sagging and swelling of voltages in sensitive loads, for example, loads used in hospitals that need a constant voltage. The DVR needs a high-performance controller. The proportional integrated-particle swarm optimization (PI-PSO) and adaptive neuro-fuzzy inference system (ANFIS) controllers were proposed for this purpose.

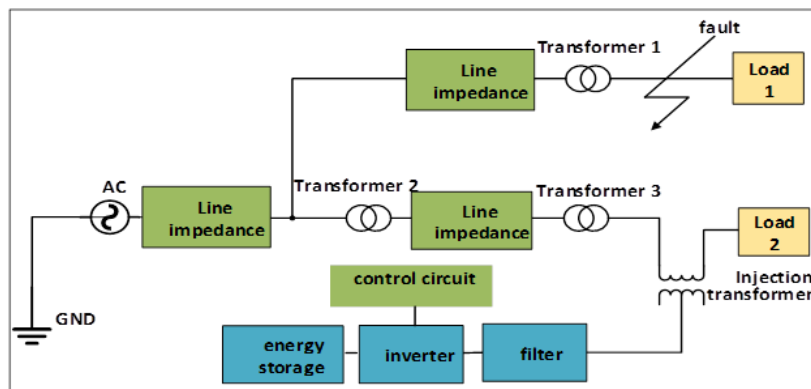


Figure 1. Single-line illustration of DVR linked in series with the feeder

2. CONSTRUCTION OF DVR

The DVR is a series-connected energy storage system that is connected to the distribution grid. Figure 1 displays the elements of a DVR. The following blocks make up the basic structure of DVR: i) voltage source inverter (VSI), ii) injection transformer, iii) passive filter, iv) energy storage unit, and v) control circuit.

2.1. Voltage source inverter

It is the foundation of a compensating device. It is responsible for converting DC to AC electricity. To build single-phase or three-phase systems, VSI uses completely regulated semiconductor power switches. insulated-gate bipolar transistors (IGBTs) are utilized in medium-power inverters, whereas GTOs or IGCTs are used in high-power inverters because of their small size and quick reaction [22], [23].

2.2. Injection transformer

It supplies the system with electrical isolation and a voltage increase. In a three-phase system, either three single-phase isolation transformers or a three-phase isolation transformer can be utilized for voltage insertion. The projected maximum output voltage must be determined when choosing an injection transformer, both technically, and economically [23].

2.3. Passive filters

A low-pass harmonic filter is employed to eliminate or keep high-frequency switching harmonics from the inverter's output as a result of applying high-frequency switching techniques. These filters can be used on the injection transformer's low voltage (LV) inverter or high voltage (HV) load sides [24].

2.4. Energy storage unit

The important purpose of these devices for energy storage is to deliver the required actual power throughout a voltage drop. Flywheels, batteries, superconducting magnetic energy storage, and super capacitors are all types of energy storage systems [25].

3. METHOD

In this section, the operating modes of the device and the methods of the control system were studied. The design of the power circuit and the control circuit was studied. The theory of PSO was studied, and the optimal values for K_p and K_i were also evaluated. The data for the ANFIS controller was studied, designed, and trained.

3.1. Operating modes of DVR

In the distribution network, a standard DVR design is employed for voltage adjustment. Operation of the DVR consists of three operation modes. Figure 2 depicts the operation mode diagram:

3.1.1. Protection mode

The bypass switches could be employed as a protective tool for safeguarding the DVR from overcurrent on the load end caused by a short circuit or significant inrush currents. The operation of the bypass switches can safeguard the DVR by providing an alternative pathway for current. Figure 2(a) demonstrates the protection mode [26].

3.1.2. Standby mode

In standby mode (typical steady-state circumstances), the DVR may either short circuit or inject a tiny voltage to mitigate voltage drops due to transformer reactance or losses. In steady state, short-circuit functioning of DVR is often chosen since modest voltage dips do not disrupt load needs provided the distributing circuit is not poor. Figure 2(b) shows the standby mode [27].

3.1.3. Injection mode

As soon as the sag is recognized, the DVR enters injection mode. For mitigation, three single-phase alternating current voltages are inserted in series with the requisite amplitude, phase, and waveform for mitigation. Figure 2(c) shows the injection mode [27].

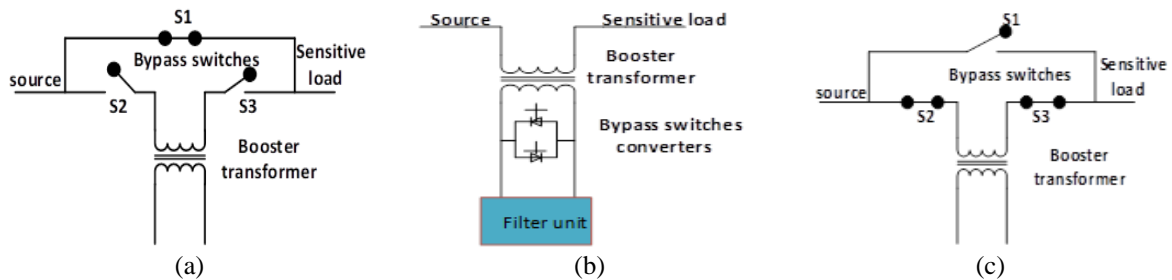


Figure 2. Operation mode diagram (a) protection mode, (b) the standby mode, and (c) the injection mode

3.2. DVR control strategies

The DVR's function is to preserve voltage quality by regulating the amplitude, form, and phase of the voltage. DVR removes voltage disruptions by restoring voltage, which entails adding the necessary energy to the line. The suggested DVR employs phase correction. In this case, the load voltage is expected to be in phase with the pre-sag voltage. Only voltage magnitude is adjusted in this suggested method. The load voltage and reference voltage are sent into the controller. Using the pulse-width modulation (PWM) approach, the controller provides pulses to the inverter based on the difference in two voltages. The inverter now emits the appropriate quantity of energy into the line through the voltage injection transformer [19]. The various DVR control techniques are shown below:

3.2.1. PI controller

The discrepancy between reference and real values is regulated by the typical PI controller. The proportional controller technique reacts rapidly, but the integral controller technique is slower but reduces the

offset between the reference and real value. Because the parts of the PI controller are calibrated by testing and the idea of true and false, the work's outcomes are less accurate [28]–[30]. The diagram of a PI controller is shown in Figure 3.

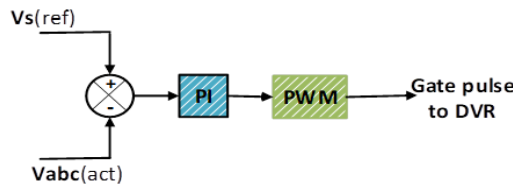


Figure 3. PI controller diagram

3.2.2. Particle swarm optimization

PSO is a population-based stochastic optimization method for solving nonlinear optimization problems. PSO is propelled along by the swarming activity of flying creatures, rushing, and fish schooling. This method excels at overcoming optimization challenges. According to its own experience, each particle seeks to update its present position and speed. Each iteration will save the best quantity achieved by each particle, which will then be compared to determine individual best amounts. Global best values can be calculated from individual best amounts. The improved controller settings were found in the last iteration's global best values [31], [32].

3.2.3. Particle swarm optimization mathematical model

Each particle (x_{ij}), whose beginning speed and location are determined at random, attempts to investigate the research space through repeated test locations in order to attain their goal using the equations given by (1), (2):

$$V_{ij}(d + 1) = W \cdot V_{ij}(d) + C_1 \cdot r_1 \cdot (P_{best\ ij} - x_{ij}(d)) + C_2 \cdot r_2 \cdot (G_{bestj} - x_{ij}(d)) \tag{1}$$

$$x_{ij}(d + 1) = V_{ij}(d + 1) + x_{ij}(d) \tag{2}$$

where $V_{ij}(d)$ is the particle i th speed in a j dimension at iteration d , $x_{ij}(d)$ is the particle i th location in a j dimension at iteration d , P_{best} is the perfect previous location of i th particle, G_{best} is the perfect particle among all the population, W is the inertia weight factor, (C_1 and C_2) are the acceleration constants, (r_1 and r_2) are the random integers between [0-1], and n is the swarm size [32], [33].

3.2.4. Adaptive neuro-fuzzy inference system controller

In a neuro-fuzzy technology, a neural network intelligence is utilized to improve the use of a fuzzy system by calculating its variables. Figure 4 show ANFIS architecture. X and Y are the inputs, f is the output, A_i and B_i are the input membership functions, and W_i is the rule firing strength.

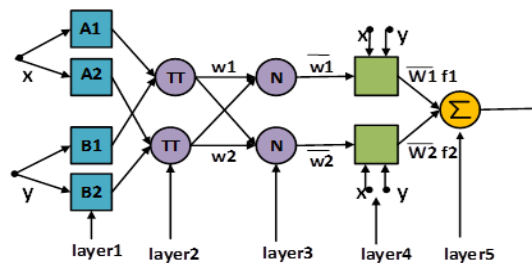


Figure 4. ANFIS architecture [24]

The ANFIS system is a hybrid of fuzzy logic and adaptable neural networks. The rule base, fuzzy sets (membership function), and inference processes are all used to build a FIS. The neuro-fuzzy design is based on the ANFIS kind, which uses the Takagi-Sugeno fuzzy inference system with a hybrid learning method. The suggested neuro-fuzzy controller is constructed, trained, and examined in the MATLAB

program using the neuro-fuzzy designer graphical user interface (GUI). The fuzzy logic approach collects and stores vast amounts of DC-link voltage data during a period in the MATLAB workspace [34]–[37].

3.3. Design and training of (ANFIS) controller

The controller is the most critical element of the DVR in voltage regulation. An ANFIS will be created. to correct for circumstances such as sag, malfunction, and swell. The ANFIS controller block diagram is shown in Figure 5. According to the ANFIS design, two vectors of error input and an error integration have been constructed. The input variables for the ANFIS controller were split into five triangle membership functions and a 25-control rule. ANFIS rule membership is shown in Figure 6. The structure of the control scheme is shown in Figure 7.

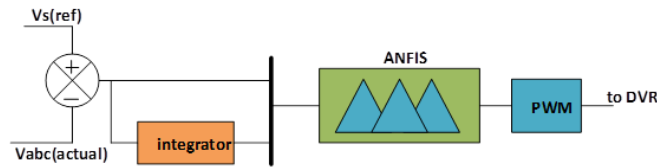


Figure 5. Block diagram of ANFIS controller

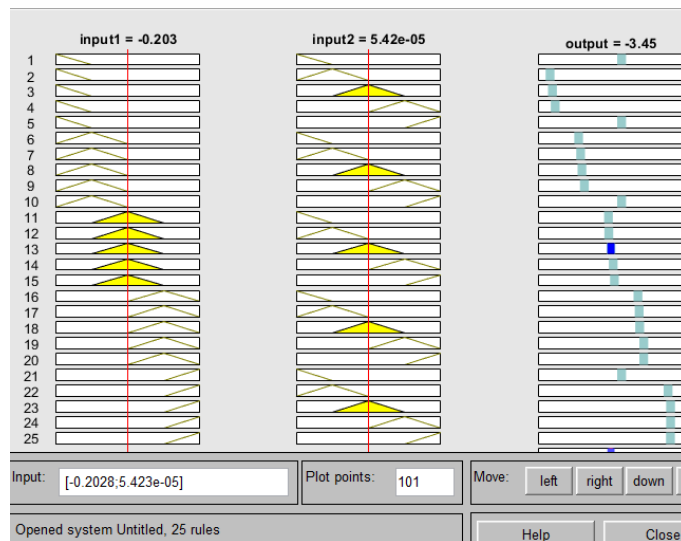


Figure 6. Rule membership

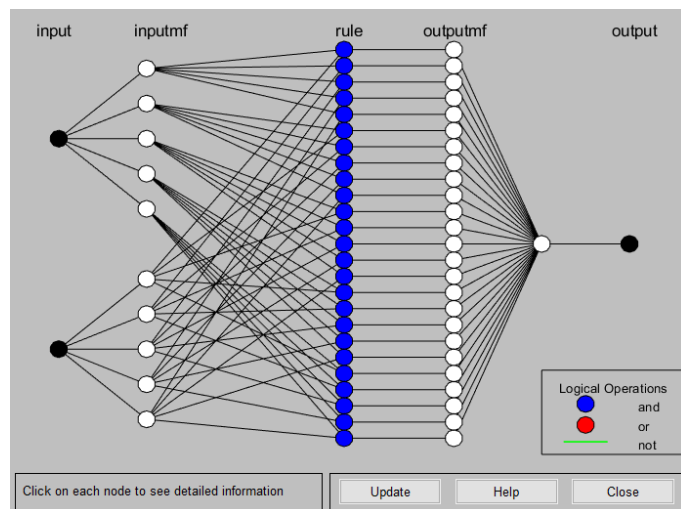


Figure 7. ANFIS model structure

3.4. Modeling and simulation

The design of the power system network with DVR is shown in Figure 8. The sag, swell, and fault development that DVR adjusts for are seen in this diagram. When there is a system failure, the load is linked to the DVR via an injection transformer and then to the network. The PSO method in this work is proposed to get the optimal values for K_p and K_i of the PI-PSO controller to minimize the fitness function (integral time absolute error). The selected values of the variables (C_1, C_2, W) of the PSO algorithm are $C_1=C_2=2, W=0.9$. The obtained minimum fitness function is 0.0000876 after 100 iterations and the PI-PSO optimal parameters are $K_P=9.957$ and $K_I=400$, while the data is being trained for the neural fuzzy technique. The DVR's control diagram is shown in Figure 9.

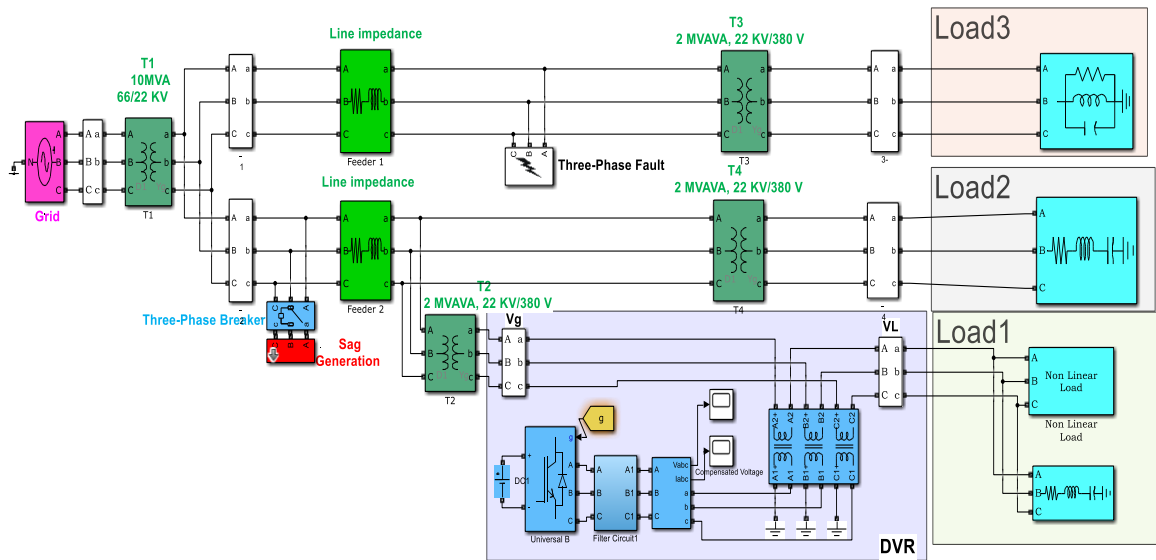


Figure 8. Modeling of the power system with DVR based on ANFIS controller

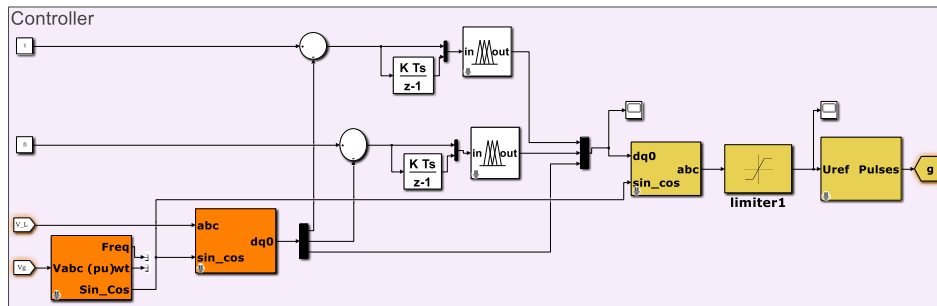


Figure 9. Control diagram of DVR

4. RESULTS AND DISCUSSION

The dynamic voltage restorer was used to protect the sensitive load in the event of various problems, such as sag and swell of the voltage, as well as when there was a malfunction in the electrical power network. The results show the problem of the voltage before compensation, the compensated voltage, and the load voltage after compensation. The results showed how important this device is for keeping the voltage at the right level.

4.1. Voltage sagging

Figure 10, which depicts the DVR's voltage injection and the associated load voltage with sag correction, shows that the grid voltage will drop by 65% between $t=0.2$ s and $t=0.5$ s. Part four in the figure shows the voltage inserted by the DVR. The DVR keeps the load voltage at pre-sag values.

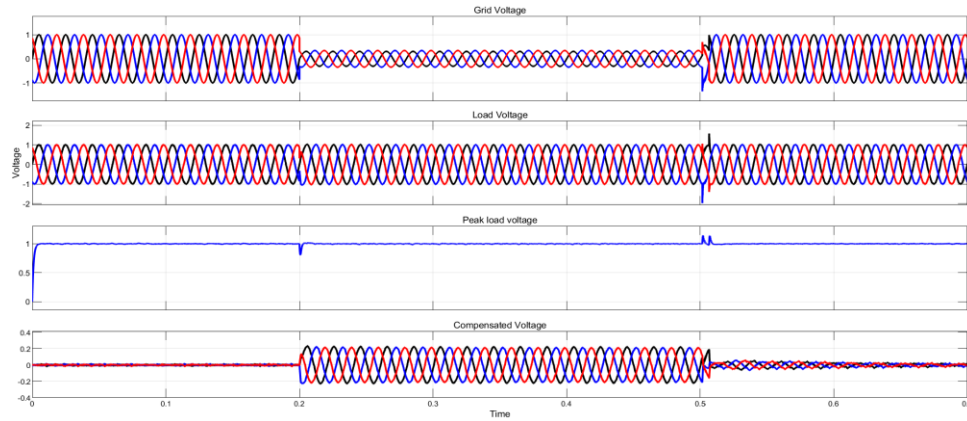


Figure 10. Three-phase sag voltage

4.2. Voltage swelling

Figure 11 displays a simulation of a 40% three-phase voltage swelling. The time spans from 0.2 to 0.5 seconds. Part four in the figure shows the voltage inserted by the DVR. The findings demonstrate that the DVR allows the load voltage to be maintained at its ideal level.

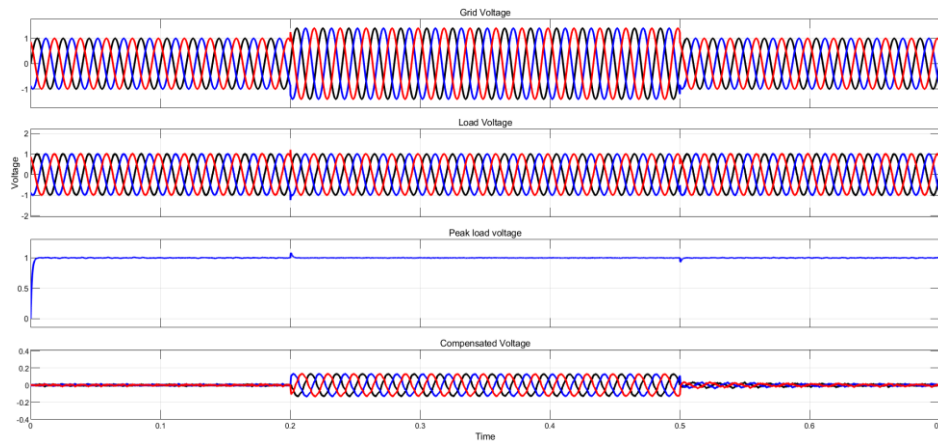


Figure 11. Three-phase swell voltage

4.3. Voltage fault

Figure 12 depicts a three-phase fault voltage that begins at 0.2 s and ends at 0.5 s. Part four in the figure shows the voltage inserted by the DVR. With the aid of the DVR, the load voltage is kept at its optimum value.

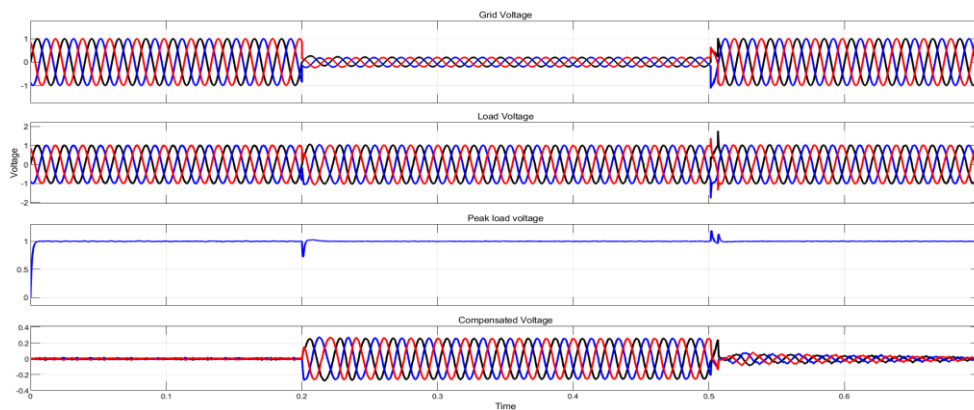


Figure 12. Three-phase fault voltage

4.4. Sag, swell, and fault voltage

Figure 13 shows the DVR-injected voltage and the corresponding load voltage, with modifications for sagging from $t=0.10$ s to $t=0.20$ s, swell from $t=0.50$ s to $t=0.60$ s, and fault from $t=0.30$ s to $t=0.40$ s. Part four in the figure shows the voltage inserted by the DVR. The load voltage remains constant due to the DVR.

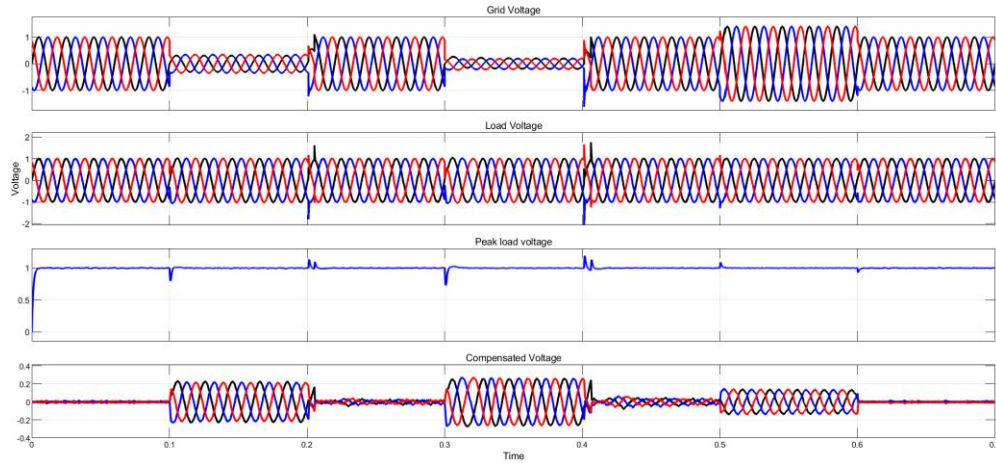


Figure 13. Three-phase sagging, swelling and fault voltage

4.5. Peak voltage

Figure 14 displays the peak value of the load voltage with different disruptions, as well as the values of overshoot, undershoot, steady state time, settling time, and integral absolute error (IAE) obtained in Tables 1 and 2 for the PI-PSO and neural fuzzy controllers, respectively. The settling time is determined at 2% of its typical value. Based on those results, the neuro fuzzy controller outperforms the PI-PSO controller, and all of the neuro fuzzy controller's results are lower than their PI-PSO counterparts, meaning that the error is decreased, there is less overshoot and undershoot, and the steady state time has enhanced.

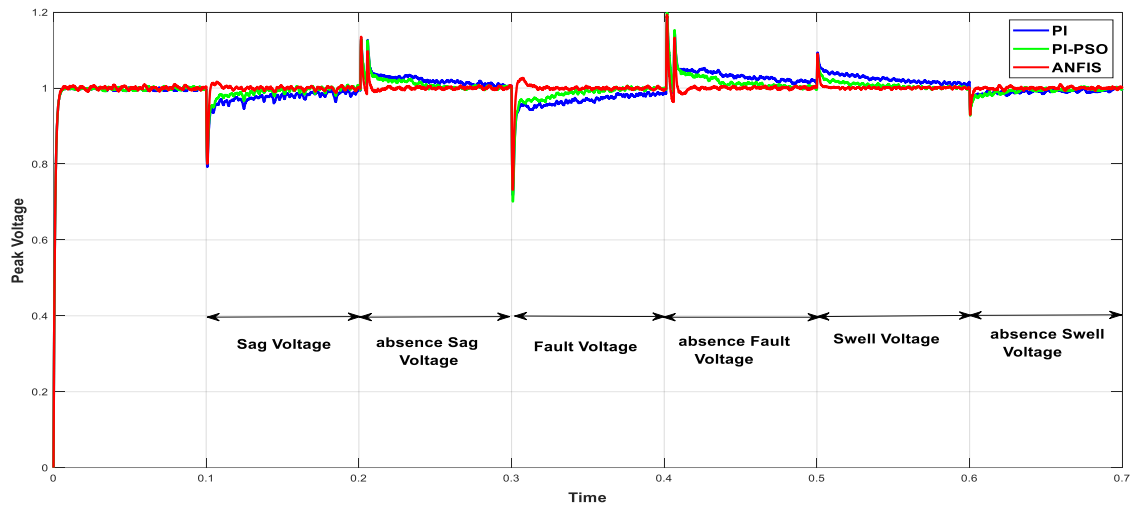


Figure 14. Peak load voltage

Table 1. PI-PSO controller peak voltage analysis

	sag	Absence sag	fault	Absence fault	swell	Absence swell
Over shoot	0	12%	0	15%	8%	0
Under shoot	20%	0	30%	0	0	10%
Steady state time	0.05	0.05	0.06	0.06	0.03	0.04
Settling time	0.008	0.004	0.02	0.007	0.004	0.006
IAE	0.0040	0.0039	0.0068	0.0073	0.0045	0.0026

Table 2. Neuro fuzzy controller peak voltage analysis

	sag	Absence sag	fault	Absence fault	swell	Absence swell
Over shoot	0	9%	0	12%	8%	0
Under shoot	20%	0%	27%	0	0	10%
Steady state time	0.01	0.01	0.01	0.01	0.003	0.004
Settling time	0.002	0.003	0.002	0.005	0.004	0.001
IAE	0.0015	0.0019	0.0016	0.0019	0.0016	0.0018

4.6. The total harmonic distortion of the load current

The simulation from FFT evaluates the THD for the load current, as shown in Figure 15. The total harmonic distortion of the load current when the ANFIS controller is utilized during the sag period is shown in Figure 15(a), whereas the total harmonic distortion of the load current when the ANFIS controller is utilized during the fault period is shown in Figure 15(b). Figure 15(c) depicts the overall harmonic distortion of the load current when the ANFIS controller is applied during the swell period. The value of THD is 6.59% for the sagging period, 6.50% for the fault period, and 6.03% for the swelling period.

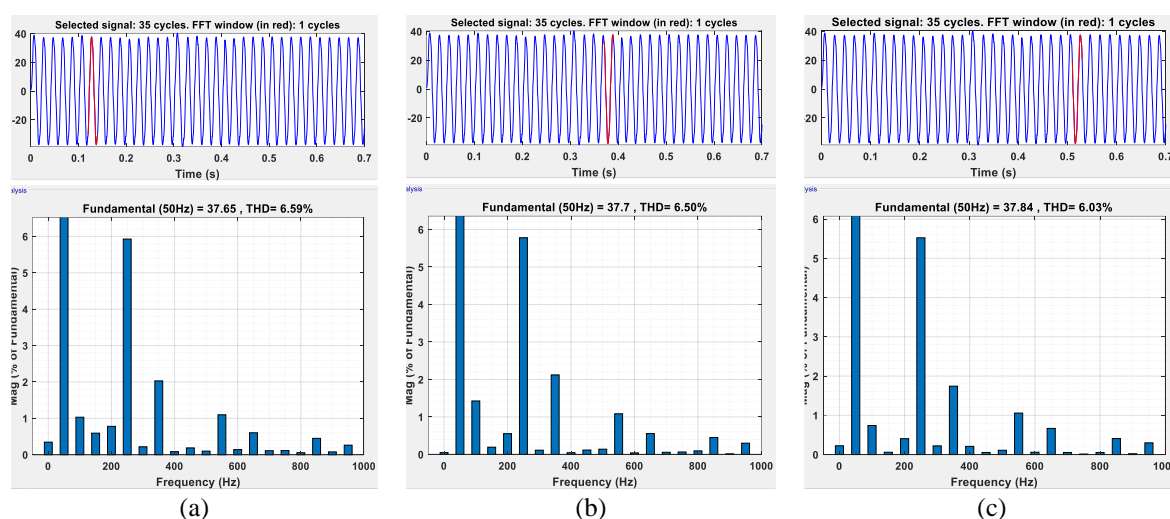


Figure 15. Frequency spectrum of load current for adaptive neuro fuzzy controller (a) sag period, (b) fault period, and (c) swell period

5. CONCLUSION

This study investigates various power quality issues utilizing DVR, such as sagging voltage, swelling voltage, and defective voltage. To tackle power issues, DVRs employ PI-PSO and ANFIS controllers. For the comparison with the ANFIS controller, regular and optimized PI controllers were employed. The ability of DVR to use an ANFIS controller confirms ANFIS functionality. In comparison to the PI and PI-PSO controllers, the ANFIS controller has less overshoot and undershoot and reaches a steady state faster. The PI also oscillates around the ultimate number. The DVR with an ANFIS outperforms the PI and PI-PSO controllers. In the case of sag voltage, the DVR with an ANFIS controller has a steady state time of (0.01) compared to (0.05) for the PI-PSO controller. For the situation of fault voltage, the DVR with an ANFIS controller has a 27% undershoot compared to 30% for the PI-PSO controller. For the absence fault voltage, the DVR with an ANFIS controller has a 12% overshoot compared to a 15% overshoot for the PI-PSO controller. For the situation of fault voltage, the DVR with an ANFIS controller has a settling time of (0.002) compared to (0.02) for the PI-PSO controller.

REFERENCES




- [1] J. Tan, X. Lin, Y. Duan, and J. Qiu, "Optimized control for a DVR to compensate long duration voltage sag with low distortion at the load," *2011 International Conference on Electrical and Control Engineering, ICECE 2011-Proceedings*, pp. 2414–2417, 2011, doi: 10.1109/ICECENG.2011.6057498.
- [2] B. Ferdi, S. Dib, B. Berbaoui, and R. Dehini, "Design and simulation of dynamic voltage restorer based on fuzzy controller optimized by ANFIS," *International Journal of Power Electronics and Drive Systems*, vol. 4, no. 2, pp. 212–222, 2014, doi: 10.11591/ijpeds.v4i2.5685.
- [3] A. B. Mohammed and M. A. M. Ariff, "The enhancement of power quality for the distribution system via dynamic voltage

- restorer,” *International Journal of Power Electronics and Drive Systems*, vol. 11, no. 3, pp. 1588–1595, 2020, doi: 10.11591/ijpeds.v11.i3.pp1588-1595.
- [4] A. B. Mohammed, M. A. M. Ariff, and S. N. Ramli, “An improved method for efficient controlling of the dynamic voltage restorer to enhance the power quality in the distribution system,” *International Journal of Power Electronics and Drive Systems*, vol. 11, no. 4, pp. 1958–1965, 2020, doi: 10.11591/ijpeds.v11.i4.pp1958-1965.
- [5] O. P. Taiwo, R. Tiako, and I. E. Davidson, “Voltage profile enhancement in low voltage 11/0.4 kV electric power distribution network using dynamic voltage restorer under three phase balance load,” *2017 IEEE AFRICON: Science, Technology and Innovation for Africa, AFRICON 2017*, pp. 991–996, 2017, doi: 10.1109/AFRCON.2017.8095617.
- [6] D. V. Chinmay and D. V. Chaitanya, “Optimum design of dynamic voltage restorer for voltage sag mitigation in distribution network,” *International Journal of Power Electronics and Drive Systems (IJPeds)*, vol. 10, no. 3, p. 1364, 2019, doi: 10.11591/ijpeds.v10.i3.pp1364-1372.
- [7] I. K. Saeed and K. Sheikhyounis, “Power quality improvement of distribution systems asymmetry caused by power disturbances based on particle swarm optimization-artificial neural network,” *Indonesian Journal of Electrical Engineering and Computer Science*, vol. 25, no. 2, pp. 666–679, 2022, doi: 10.11591/ijeecs.v25.i2.pp666-679.
- [8] M. Zadehbagheri, T. Sutikno, and R. Ildarabadi, “Using y-source network as a connector between turbine and network in the structure of variable speed wind turbine,” *International Journal of Power Electronics and Drive Systems*, vol. 12, no. 3, pp. 1644–1658, 2021, doi: 10.11591/ijpeds.v12.i3.pp1644-1658.
- [9] P. U. Rani, “Voltage swell compensation in an interline dynamic voltage restorer,” *Journal of Scientific and Industrial Research*, vol. 73, no. 1, pp. 29–32, 2014.
- [10] S. Suraya, P. Sujatha, and P. B. Kumar, “Contemporary control of DG Integrated DVR for Sag swell and harmonic mitigation,” *International Journal of Electrical and Computer Engineering*, vol. 8, no. 5, pp. 2721–2730, 2018, doi: 10.11591/IJECE.V8I5.PP2721-2730.
- [11] S. A. Rahman and E. Dagnev, “Voltage sag compensation using direct converter based DVR by modulating the error signal,” *Indonesian Journal of Electrical Engineering and Computer Science*, vol. 19, no. 2, pp. 608–616, 2020, doi: 10.11591/ijeecs.v19.i2.pp608-616.
- [12] T. Toumi, A. Allali, O. Abdelkhalek, A. Ben Abdalkader, A. Meftouhi, and M. A. Soumeur, “PV integrated single-phase dynamic voltage restorer for sag voltage, voltage fluctuations and harmonics compensation,” *International Journal of Power Electronics and Drive Systems*, vol. 11, no. 1, pp. 545–554, 2020, doi: 10.11591/ijpeds.v11.i1.pp547-554.
- [13] M. F. Kangarlu, E. Babaei, and F. Blaabjerg, “A comprehensive review of dynamic voltage restorers,” *International Journal of Electrical Power and Energy Systems*, vol. 92, pp. 136–155, 2017, doi: 10.1016/j.ijepes.2017.04.013.
- [14] S. A. Rahman and G. Teshome, “Maximum voltage sag compensation using direct converter by modulating the carrier signal,” *International Journal of Electrical and Computer Engineering*, vol. 10, no. 4, pp. 3936–3941, 2020, doi: 10.11591/ijece.v10i4.pp3936-3941.
- [15] A. Javadian, M. Zadehbagheri, M. J. Kiani, S. Nejatian, and T. Sutikno, “Modeling of static var compensator-high voltage direct current to provide power and improve voltage profile,” *International Journal of Power Electronics and Drive Systems*, vol. 12, no. 3, pp. 1659–1672, 2021, doi: 10.11591/ijpeds.v12.i3.pp1659-1672.
- [16] A. Athamneh and B. A.-. Majali, “Voltage stability enhancement for large scale squirrel cage induction generator based wind turbine using statcom,” *International Journal of Power Electronics and Drive Systems*, vol. 12, no. 3, pp. 1784–1794, 2021, doi: 10.11591/ijpeds.v12.i3.pp1784-1794.
- [17] A. B. Mohammed, M. A. M. Ariff, and S. N. Ramli, “Power quality improvement using dynamic voltage restorer in electrical distribution system: An overview,” *Indonesian Journal of Electrical Engineering and Computer Science*, vol. 17, no. 1, pp. 86–93, 2019, doi: 10.11591/ijeecs.v17.i1.pp86-93.
- [18] M. N. Tandjaoui, C. Benachaiba, O. Abdelkhalek, M. L. Doumbia, and Y. Mouloudi, “Sensitive loads voltage improvement using Dynamic Voltage Restorer,” *Proceedings of the 2011 International Conference on Electrical Engineering and Informatics, ICEEI 2011*, no. July, 2011, doi: 10.1109/ICEEI.2011.6021679.
- [19] S. V. R. L. Kumari and M. U. Vani, “Analysis of various control strategies of dynamic voltage restorer for power quality improvement in distribution system,” *ARPN Journal of Engineering and Applied Sciences*, vol. 14, no. 12, pp. 2211–2218, 2019.
- [20] I. I. A.-. Naimi, J. A. Ghaeb, M. J. Baniyounis, and M. A.-. Khawaldeh, “Fast detection technique for voltage unbalance in three-phase power system,” *International Journal of Power Electronics and Drive Systems*, vol. 12, no. 4, pp. 2230–2242, 2021, doi: 10.11591/ijpeds.v12.i4.pp2230-2242.
- [21] A. I. Omar, S. H. E. A. Aleem, E. E. A. El-Zahab, M. Algablawy, and Z. M. Ali, “An improved approach for robust control of dynamic voltage restorer and power quality enhancement using grasshopper optimization algorithm,” *ISA Transactions*, vol. 95, pp. 110–129, 2019, doi: 10.1016/j.isatra.2019.05.001.
- [22] W. A. A. Saleh, N. A. M. Said, W. A. Halim, and A. Jidin, “Comparison between selective harmonic elimination and nearest level control for transistor clamped H-bridge inverter,” *Indonesian Journal of Electrical Engineering and Computer Science*, vol. 6, no. 1, pp. 46–55, 2022, doi: 10.11591/ijeecs.v26.i1.pp46-55.
- [23] P. Verma and R. Thakur, “Review on dynamic voltage restorer based fuzzy logic controller,” vol. 6, no. 4, pp. 4–7, 2020.
- [24] R. Topologies and P. Converters, “Control Methods , and Modified Configurations,” 2020.
- [25] D. V. Tien, R. Gono, and Z. Leonowicz, “A multifunctional dynamic voltage restorer for power quality improvement,” *Energies*, vol. 11, no. 6, pp. 1–17, 2018, doi: 10.3390/en11061351.
- [26] S. Kumar, “Modelling and simulation of DVR using fuzzy logic control,” vol. 3, no. 02, pp. 53–60, 2016.
- [27] M. Tumay, a Teke, K. Bayindir, and M. Cuma, “Simulation and modeling of a dynamic voltage restorer,” *Proceeding of the 4th, 2005*.
- [28] S. Kasa and S. Ramasamy, “Photovoltaic fed dynamic voltage restorer with voltage disturbance mitigation capability using ANFIS controller,” *International Journal of Renewable Energy Research*, vol. 6, no. 3, pp. 825–832, 2016.
- [29] M. Bahy, A. S. Nada, S. H. Elbanna, and M. A. M. Shanab, “Voltage control of switched reluctance generator using grasshopper optimization algorithm,” *International Journal of Power Electronics and Drive Systems*, vol. 11, no. 1, pp. 75–85, 2020, doi: 10.11591/ijpeds.v11.i1.pp75-85.
- [30] M. Chiranjivi and K. Swarnasri, “A novel optimization-based power quality enhancement using dynamic voltage restorer and distribution static compensator,” *Indonesian Journal of Electrical Engineering and Computer Science*, vol. 6, no. 1, pp. 160–171, 2022, doi: 10.11591/ijeecs.v26.i1.pp160-171.
- [31] K. Jeyaraj, D. Durairaj, and A. I. S. Velusamy, “Development and performance analysis of PSO-optimized sliding mode controller-based dynamic voltage restorer for power quality enhancement,” *International Transactions on Electrical Energy Systems*, vol. 30, no. 3, pp. 1–14, 2020, doi: 10.1002/2050-7038.12243.




- [32] E. Chetouani, Y. Errami, A. Obbadi, and S. Sahnoun, "Optimal tuning of pi controllers using adaptive particle swarm optimization for doubly-fed induction generator connected to the grid during a voltage dip," *Bulletin of Electrical Engineering and Informatics*, vol. 10, no. 5, pp. 2367–2376, 2021, doi: 10.11591/eei.v10i5.2843.
- [33] S. S. Salman, A. T. Humod, and F. A. Hasan, "Optimum control for dynamic voltage restorer based on particle swarm optimization algorithm," *Indonesian Journal of Electrical Engineering and Computer Science*, vol. 26, no. 3, p. 1351, 2022, doi: 10.11591/ijeecs.v26.i3.pp1351-1359.
- [34] C. Bukata, "Anfis based power quality solution using unified power quality," *Bayero Journal of Engineering and Technology*, vol. 12, no. 2, 2017.
- [35] W. Suparta and W. S. Putro, "Comparison of tropical thunderstorm estimation between multiple linear regression, Dvorak, and ANFIS," *Bulletin of Electrical Engineering and Informatics*, vol. 6, no. 2, pp. 149–158, 2017, doi: 10.11591/eei.v6i2.648.
- [36] M. Y. Suliman, "Voltage profile enhancement in distribution network using static synchronous compensator STATCOM," *International Journal of Electrical and Computer Engineering*, vol. 10, no. 4, pp. 3367–3374, 2020, doi: 10.11591/ijece.v10i4.pp3367-3374.
- [37] A. J. Ali, M. Y. Suliman, L. A. Khalaf, and N. S. Sultan, "Performance investigation of stand-alone induction generator based on STATCOM for wind power application," *International Journal of Electrical and Computer Engineering*, vol. 10, no. 6, pp. 5570–5578, 2020, doi: 10.11591/ijece.v10i6.pp5570-5578.

BIOGRAPHIES OF AUTHORS






Saddam Subhi Salman    was born in Baghdad, Iraq in 1981. He received a Bachelor's degree in Electrical Engineering from University of Baghdad, Iraq in 2005. He is currently studying toward a Master's degree of Science in Electrical Power Engineering at the University of Technology, Iraq. He can be contacted at email: eee.20.53@grad.uotechnology.edu.iq.



Prof. Dr. Abdulrahim Thiab Humod    was born in Baghdad, Iraq, in 1961. He received his B.Sc. in the Department of Electrical and Electronic Engineering, Military engineering college, Iraq, respectively in 1984. He received his M.Sc in 1990 (control and guidance) from the Military engineering college, Iraq. His Ph.D. from Military engineering college (control and guidance) He is now a Professor in University of Technology, Iraq. He researches interests are control and guidance. He can be contacted at email: 30040@uotechnology.edu.iq.



Asst. Prof. Dr. Fadhil A. Hasan    was born in Baghdad, Iraq in February 17, 1970. He received the B.Sc. from the university of Al-Mustansiryah, Baghdad, Iraq, in 1991, in electrical engineering. He received the M.Sc. and Ph.D. degrees from University of Technology, in 2008 and 2017 respectively, in electrical machine and control engineering. In 2008, he joined the Department of Electrical Engineering at University of Technology, Baghdad, in Iraq, as an Asst. Lecturer. Currently he is an Asst. Prof. in the Department of Electrical Engineering at University of Technology, Baghdad, in Iraq. He has published over 22 refereed journal and conference papers in the areas of induction heating, control systems, power electronics, and electrical machine. He can be contacted at email: 30077@uotechnology.edu.iq.